Title

High-resolution qualitative and quantitative magnetic resonance evaluation of the glenoid labrum

Journal

Journal of Computer Assisted Tomography, 39(6)

ISSN

0363-8715

Authors

Iwasaki, K
Tafur, M
Chang, EY
et al.

Publication Date

2015

DOI

10.1097/RCT.0000000000000307

HHS Public Access

Author manuscript

J Comput Assist Tomogr. Author manuscript; available in PMC 2016 November 01.

Published in final edited form as:

J Comput Assist Tomogr. 2015 ; 39(6): 936–944. doi:10.1097/RCT.0000000000000307.

High Resolution Qualitative and Quantitative MR Evaluation of the Glenoid Labrum

Kenyu Iwasaki, M.D., Ph.D.[1], **Monica Tafur, M.D.**[1], **Eric Y. Chang, M.D.**[2,1], **SherondaStatum, M.S.**[1], **Reni Biswas, B.S.**[1], **Betty Tran, B.S.**[1], **Won C. Bae, Ph.D.**[1], **Jiang Du, Ph.D.**[1], **Graeme M. Bydder, M.B., Ch.B.**[1], and **Christine B. Chung, M.D.**[1,1]

Kenyu Iwasaki: kenyu510@icloud.com; Monica Tafur: motafur@gmail.com; SherondaStatum: sherondastatum@msn.com; Reni Biswas: biswas.reni@gmail.com; Betty Tran: tranbetty90@gmail.com; Won C. Bae: wbae@ucsd.edu; Graeme M. Bydder: gbydder@ucsd.edu; Christine B. Chung: cbchung@ucsd.edu

[1]Department of Radiology, University of California, San Diego, San Diego, California, United States

[2]Radiology Service, VA San Diego Healthcare System, San Diego, California, UnitedStates

Abstract

Objective—To implement qualitative and quantitative MR sequences for the evaluation of labral pathology.

Methods—Six glenoid labra were dissected and the anterior and posterior portions were divided into normal, mildly degenerated, or severely degenerated groups using gross and MR findings. Qualitative evaluation was performed using T1-weighted, proton density-weighted (PD), spoiled gradient echo (SPGR) and ultra-short echo time (UTE) sequences. Quantitative evaluation included T2 and T1rho measurements as well as T1, T2*, and T1rho measurements acquired with UTE techniques.

Results—SPGR and UTE sequences best demonstrated labral fiber structure. Degenerated labra had a tendency towards decreased T1 values, increased T2/T2* values and increased T1 rho values. T2* values obtained with the UTE sequence allowed for delineation between normal, mildly degenerated and severely degenerated groups ($p<0.001$).

Conclusion—Quantitative T2* measurements acquired with the UTE technique are useful for distinguishing between normal, mildly degenerated and severely degenerated labra.

Introduction

The glenoid labrum is a vascularized rim of fibrous tissue that outlines the bony glenoid[1]. It plays an important role in deepening the glenoid fossa and increases the articulating surface area of the glenoid to help prevent glenohumeral instability. The glenoid labrum contributes approximately one-third to one-half of the total depth of the socket[1]. The labrum also has other important functions, including acting as a cushion to protect the chondral surface[2],

Corresponding Author: Eric Y. Chang, MD, 3350 La Jolla Village Drive, MC 114, San Diego, CA 92161, ericchangmd@gmail.com, Office: (858)552-8585 x7656, Fax: (858)642-6356.

Conflict of Interest

The authors declare that there is no conflict of interest

providing a valve-effect that maintains negative intra-articular pressure to secure further stability, facilitating nutritional delivery to the glenoid cavity, maintaining joint lubrication, and acting as an attachment site for several structures such as the glenohumeral ligaments and the long head of the biceps tendon[1, 3].

The core structure of the labrum is composed of collagen fiber bundles that run in a circumferential orientation around the glenoid rim. These circumferential collagen fibers intermingle with radially orientated fibers at the biceps tendon insertion[2, 4]. The majority of collagen fibrils are composed of type I collagen, but type II collagen is also present in a smaller amount[5].

The labrum appears dark on conventional MR images due to the short T2 relaxation time, similar to the calcified layer of cartilage, the meniscus and myriad of other short T2 tissues within the musculoskeletal system[6, 7]. Numerous studies have demonstrated a moderate to high degree of accuracy for the diagnosis of labral tears using non-contrast MRI[8, 9], CT arthrography[10], indirect MR arthrography[11] and direct MR arthrography[12]. However, all of the previously utilized imaging approaches are limited for the diagnosis of early labral degeneration due to poor tissue contrast within the labrum. Although MRI has traditionally been thought of as having superior soft tissue contrast, conventional sequences tailored for long T2 tissues can be limited for the delineation between normal versus degenerated labral tissue due to the relatively short T2 relaxation times. Furthermore, there is no opportunity for quantification of short T2 tissues using conventional sequences.

With the development of ultra-short echo time (UTE[6, 13–15]) MR imaging, there is now the potential for direct qualitative evaluation of structures with a majority of short T2 components. In addition, clinically-compatible quantitative measurements of nuclear magnetic resonance relaxation can now be performed on these short T2 tissues, including T1[16], T2*[17], and T1rho[14]. These sequences have established efficacy in the characterization of tissue infrastructure as well as the ability to detect early structural alteration in both the calcified layer of articular cartilage and in the meniscus.

Despite the increasing interest in quantitative MRI in the musculoskeletal system, there has been no previous application to labral tissue. The objective of this study is to implement qualitative and quantitative MR pulse sequences tailored for short T2 tissues for the evaluation of labral structure and pathology.

Materials and Methods

Specimen preparation

This cadaveric study was approved by our Institutional Review Board. Six cadaveric shoulders were obtained from the Donor Program of our institution within 24 hours of death. The specimens were allowed to thaw for 24 hours at room temperature prior to dissection and imaging. Age range at death was from 41 to 94 years (4 female and 2 male; average age, 74 years). An orthopedic surgeon with 7 years of experience performed the entire dissection. The latissimus dorsi and deltoid muscles were removed from the scapula, clavicle and humerus. The rotator cuff was cut off proximally and the glenohumeral joint capsule was

incised carefully, avoiding damage to the labrum. The neck of the scapula was osteotomized using a handsaw. The harvested sample included the glenoid labrum, the glenoid fossa and the proximal attachment of the long head of biceps.

Gross Inspection

All specimens were carefully reviewed with emphasis on the anterior and posterior labrum. The severity of labral pathology was classified based upon visual inspection and palpation of the gross specimen using a classification as follows: specimens with no findings of labral or chondral pathology were classified as “normal”, specimens with degeneration of the glenoid labrum were classified as “degenerated”, and specimens in which both the glenoid labrum and the articular cartilage were degenerated were classified as “osteoarthritis” (Figure 1).

MR imaging

All scans were performed on a 3-T Signa TwinSpeed scanner (GE Healthcare Technologies, Milwaukee, WI) with a 3-inch single-channel surface coil. The sample was oriented with the longitudinal axis of the glenoid fossa (an axis extending from the inferior portion of the glenoid fossa to its superior portion) parallel to the main magnetic field (B0). High-resolution qualitative sequences included: T1-weighted spin echo (SE), proton density-weighted (PD) SE, 2D/3D spoiled gradient echo (SPGR)[18, 19] and 2D/3D ultra-short echo time (UTE)[13-15]. For quantification, T1, T2, T2*, and T1rho measurements were performed. Specifically, quantitative sequences included T1 measurements acquired using a saturation recovery technique and UTE acquisition[16, 20], T2 measurements acquired with a Carr-Purcell-Meiboom-Gill (CPMG) technique[21, 22], T2* measurements acquired with a multi-echo UTE acquisition[17], and T1rho measurements acquired with 2D[23], 3D[24], and UTE acquisitions[14, 25]. Typical acquisition parameters are presented in Table 1.

MR Imaging Analysis

Two subspecialized musculoskeletal radiologists with 4 and 16 years of experience reviewed and graded the labrum on the qualitative and quantitative sequences. Anterior and posterior labral morphology and signal intensity was assessed to determine the presence or absence of degeneration and the degree of pathology. The severity of labral pathology on MR imaging was assessed using a staging system as follows. Stage 0 included normal labra. A normal labrum demonstrated homogeneously low signal intensity on all T1 and PD sequences, without any findings of degeneration, tear or detachment. Stage 1 included a torn or detached labrum. Stage 2 included partially degenerated labra. Stage 3 included completely degenerated labra. Stage 4 included completely degenerated labra associated with degenerative changes in the adjacent glenoid cartilage (Figure 2).

Two ROIs were drawn in each specimen (in the anterior and posterior labrum) for each quantitative sequence and both global values and pixel-by-pixel maps were determined based on signal intensity utilizing a nonlinear least square mono-exponential curve fitting program in MATLAB (The MathWorks, R2011b). Values from the 12 ROIs analyzed were categorized in 3 groups according with the morphologic staging on MR images above: normal (Stage 0), mild degeneration (Stages 1 and 2) and severe degeneration (Stage 3 and 4). Mean T1, T2, UTE T2*, UTE T1rho, 2D T1rho and 3D T1rho values were obtained for

each group, and were compared to determine differences among normal, mild degeneration and severe degeneration.

Statistical Analysis

The values obtained from quantitative MRI were analyzed using unpaired Student t-test, ANOVA and posthoc Tukey test. Differences between groups with p-values of less than 0.05 were considered to be statistically significant. All of the statistical analyses were performed using the Systat program (version 10, Sysat Software Inc., San Jose, CA).

Results

Findings at Gross Inspection

Three ROIs were classified as normal, four ROIs were classified as degeneration of labrum and 5 ROIs were classified as osteoarthritis (Table 2). In general, degenerated labral tissue was irregular and its color appeared reddish or whitish (Figure 3A, 3B and 3C).

Findings at MR Imaging

The MR classification system for labral pathology was approximately consistent with the classification at the gross inspection. On high-resolution qualitative MR imaging, three ROIs appeared normal (stage 0) and the other 9 ROIs appeared degenerated. Two ROIs were classified as stage 2, two ROIs were classified as stage 3 and five ROIs were classified as stage 4. No labral were classified as stage 1 (Table 2). Axial SPGR MR images clearly demonstrated labral morphology and signal intensity allowing staging of labral pathology (Figure 3D, 3E and 3F).

Qualitative MR Imaging

Internal structure of the labrum was well demonstrated on the high-resolution MR images. On T1-weighted sequences, the normal labrum appeared homogeneously hypointense, whereas it had intermediate to high signal intensity on SPGR and UTE sequences. The glenoid attachment of the labrum and the labrum-cartilage interface are well demonstrated on axial high-resolution MR images, especially using the UTE sequences which provided better contrast and allowed for the differentiation between fibrocartilaginous matrix and collagen fiber structure as compared with the other sequences. Focal areas of increased signal intensity secondary to magic angle effects are demonstrated where the collagen fibers of the labrum are located at 55° of B0 on sagittal high-resolution MR images (Figure 4).

The fibrocartilaginous matrix of the normal labrum was best depicted using very short TEs (0.03 ms) whereas the fiber structure was better demonstrated using slightly longer TEs (6.6 ms) where the contrast between both components was greater. As TE increases, signal from both the fibrocartilaginous matrix and the area of alteration start to decay, appearing hypointense. Therefore, it was difficult to differentiate these tissues, especially with longer TEs (13.2 ms and 20 ms) (Figure 5).

Quantitative MR Imaging

The results of high-resolution quantitative MR imaging of normal and degenerated labra are illustrated in Figure 6 using mono-exponential fitting curves and color maps. T2 CPMG, UTE T2*, 2D/3D T1rho and UTE T1rho sequences showed increased signal intensity in the degenerated labrum as compared with the normal labrum. This is reflected in the mono-exponential fitting curves and the color mapping where the degenerated labra have higher T2, T2* and T1rho values.

The mean values from 3 groups (normal, mild degeneration and severe degeneration) are shown in Figure 7. The range of T1 values obtained from the TSR sequence was 564.9 to 1424.9 ms (mean 787.2 ms ± 302.4). There was shortening of mean T1 values in mildly and severely degenerated labra (600.7 ± 47.3 ms and 702.0 ± 138.9 ms respectively) as compared with the normal labra (1110.3 ms ± 476.6 ms). The difference between degenerated (mild + severe) labra and normal labra was significant ($p = 0.0237$), however the difference between three groups was not significant ($p = 0.0790$).

The T2 values ranged from 8.9 to 26.3 ms (mean 21.9 ± 4.5 ms). There was an increase in the mean T2 values in mildly and severely degenerated labra (23.7 ± 1.2 ms and 23.4 ± 2.2 ms respectively) as compared with the normal labra (17.4 ± 7.3 ms). The difference between degenerated (mild + severe) labra and normal labra was significant ($p = 0.0339$), however the difference between three groups was not significant ($p = 0.1192$).

The range of UTE T2* values obtained was 2.1 to 15.1 ms (mean 7.4 ms ± 3.9). In this case a highly significant difference was found when comparing normal with degenerated (mild + severe) labra ($p = 0.0068$). The UTE T2* values gradually increased with advancing degeneration with mean UTE T2* values of 2.7 ± 0.7 ms in normal labra, 4.9 ± 0.9 ms in mildly degenerated labra and 10.1 ± 2.3 ms in severely degenerated labra. The difference between three groups was highly significant ($p = 0.0008$).

The mean T1rho values obtained from the 2D T1rho sequence ranged from 10.7 to 33.0 ms (mean 19.7 ± 6.9 ms). The mean T1rho values were increased in the severely degenerated labra (24.0 ± 5.4 ms) as compared with the normal or mildly degenerated labra, which had similar T1rho values (13.7 ± 4.4 ms and 13.8 ± 4.3 ms respectively). The difference between three groups was significant ($p = 0.0226$), However, when comparing normal with degenerated (mild + severe) labra, the difference was not significant ($p = 0.0882$).

The mean T1rho values obtained from the 3D T1rho sequence were overall comparable with the values obtained from the 2D T1rho sequence. T1 rho values ranged from 9.6 to 32.3 ms (mean 17.3 ± 6.6 ms). The mean T1rho value in severely degenerated labra was increased (21.2 ± 5.9 ms) as compared with the mean values in the normal or mildly degenerated groups (11.8 ± 1.2 ms and 11.9 ± 3.3 ms respectively). The difference between three groups was significant ($p = 0.0332$), However, when comparing normal with degenerated (mild + severe) labra, the difference was not significant ($p = 0.0973$).

The range of UTE T1rho values obtained was 5.6 to 15.8 ms (mean 9.6 ms ± 3.1). In this case a significant difference was found when comparing normal with degenerated (mild +

severe) labra (p = 0.0314). The UTE T1rho values gradually increased with advancing degeneration with mean UTE T1rho values of 6.4 ± 1.2 ms in normal labra, 8.0 ± 2.8 ms in mildly degenerated labra and 11.4 ms ± 2.4 ms in severely degenerated labra. The difference between three groups was significant (p = 0.0239).

Discussion

In the present study, we successfully implemented qualitative sequences including 2D SGPR, 3D SPGR, 2D UTE and 3D UTE sequences on the glenoid labrum for the purpose of characterizing internal fiber structure. SPGR sequences have been used to detect early articular cartilage disease because it produces bright cartilage signal[19, 26]. In recent years both 2D and 3D UTE sequences have been developed to image short T2 tissues such as calcified cartilage[13], menisci[15, 27] and Achilles tendon[14]. But, to our knowledge, there have been no reports applying the UTE sequence for evaluation of the glenoid labrum. As expected, the signal intensity of the labrum was higher on UTE sequences as compared with T1 and PD sequences. We found that UTE sequences provided better contrast, allowing the differentiation between fibrocartilaginous matrix and collagen fiber structure as compared with the SPGR sequence and conventional spin-echo sequences such as T1-weighted and PD-weighted sequences. We demonstrate that UTE sequences are useful for the evaluation of the fibrocartilaginous matrix of the normal labrum.

Quantitative MR imaging has been reported to be sensitive to structural alteration in short-T2 tissues[27]. Several articles published in the literature have demonstrated that T2, T2* and T1rho relaxation times increase with tissue degeneration, where water content and mobility increases and collagen disorganizes[2, 28]. To our knowledge, no study has implemented quantitative MR imaging to evaluate the glenoid labrum.

In short T2, collagen-rich tissues, such as ligaments and menisci, macromolecular structure restricts proton mobility and causes rapid T2 relaxation. As a result, with the TEs used in conventional clinical imaging, little or no signal is acquired. With UTE pulse sequences, TEs below 0.2 ms can be achieved[27]. In the present study, we have found that T2* measurements acquired with the UTE technique was more sensitive compared with the other quantitative sequences in terms of both identifying the presence of labral degeneration and evaluating the progression of degeneration. Quantitative UTE T2* measurements may be a promising technique with regards to diagnosing labral pathology at an early stage, evaluating the progression of degeneration, and for the monitoring of therapeutic efficacy.

T1 relaxation time measurements have been performed on many tissues[16]. It has been reported that degenerated lumber discs had lower T1 values as compared with normal ones[29]. In the present study, mildly degenerated labra had decreased T1 values as compared with normal labra. However, no significant differences were detected between mildly and severely degenerated labra. T1 values have been reported to reflect water content in some tissues. However, the sensitivity for detection of articular cartilage degeneration is low with T1 mapping, although it is improved after gadolinium infusion (delayed gadolinium enhanced MRI of cartilage: dGEMRIC)[30]. Our results also suggest that T1 measurements may be limited for the evaluation of degenerated labra.

T2 measurements are another commonly used tool for measuring water content as well as collagen integrity and orientation. Increased T2 relaxation time is correlated with histological degeneration of articular cartilage[21]. In the present study, degenerated (mild + severe) labra had increased T2 values as compared with normal labra. However, there was almost no difference between mildly and severely degenerated labra. Since labra have short T2 values (about 10 to 25 ms), T2 mapping using spin-echo sequences and routinely used TEs (ranging from 10 to 80 ms) may have less sensitivity compared with TEs that can be achieved using UTE sequences (TE < 0.2 ms).

In articular cartilage and menisci, T1rho values have been considered to reflect the degree of degeneration. In particular, it has been inversely correlated with proteoglycan and glycosaminoglycan[31, 32]. The concentrations of proteoglycan in hyaline cartilage and meniscus were reported to be 5–10% and 1–2% respectively[33]. However, the concentration of proteoglycan in labrum has not been reported, and similarly the concentrations with degeneration are unknown. UTE T1rho is a novel sequence that combines a spin-lock pulse with the UTE acquisition. This sequence allows for the measurement of T1rho in short T2 tissues, including the Achilles tendon and the meniscus[14, 32]. In the present study, T1rho was measured with three different methods. Specifically, the 2D spiral chopped magnetization preparation (SCMP)[34], 3D magnetization-prepared angle-modulated partitioned k-space spoiled gradient echo snapshots (MAPSS)[24] and 2D UTE methods were employed. For the 2D SCMP and 3D MAPSS T1rho sequences, severely degenerated labra had significantly higher T1rho values compared with normal and mildly degenerated labra, however, there was almost no difference between normal and mildly degenerated labra. For the UTE T1rho sequence, there were significant differences between all three groups. UTE T1rho may be a useful technique with regards to the detection of early stage degeneration and for the evaluation of the progression of degeneration.

There are several limitations to this pilot study. Firstly, only six cadaveric shoulder specimens were studied. However, ours is a pilot study implementing quantitative sequences for the first time on the labrum and based on the group effect sizes, power analyses can be performed for future studies. All of the sequences used in this study have been translated into patients in previously published studies, and based on our results, use of the quantitative UTE T2* sequence may be the most useful for future in vivo studies. Secondly, histological evaluation was not implemented. However, we utilized both an MR classification system for labral pathology and gross inspection (a surgical standard), and both were approximately consistent with each other. A third limitation is the magic angle effect, which is due to the highly ordered structure of collagenous tissues and dipole–dipole interaction[35]. In the present study, focal areas of increased signal intensity secondary to magic angle effects were observed on sagittal MR slices where the collagen fibers of the labrum are located at 55° with respect to B0. However, our ROIs were carefully chosen at regions where collagen bundles would be expected to be 90° with respect to B0, thereby reducing the magic angle effect.

In conclusion, we have successfully performed high-resolution qualitative and quantitative techniques on cadaveric labra using UTE techniques. High-resolution SPGR and 2D/3D UTE sequences were more useful in depicting the internal fiber structure of the labrum as

compared with conventional sequences where longer TEs were used. Quantitative MR imaging reflected the qualitative findings with increased T2, T2*, T1rho relaxation times with advancing labral degeneration. UTE T2* measurements were more sensitive than the other quantitative sequences, which may be a promising technique for diagnosing labral pathology at the early stage, evaluating the progression of degeneration, and monitoring therapeutic efficacy.

Acknowledgments

Funding

The authors acknowledge funding from the National Institutes of Health grant #5R01DE022068 and from the VA Clinical Science Research and Development Service Career Development Award #IK2CX000749.

References

1. Levine WN, Flatow EL. The pathophysiology of shoulder instability. Am J Sports Med. 2000; 28:910–917. [PubMed: 11101119]
2. Nishida K, Hashizume H, Toda K, et al. Histologic and scanning electron microscopic study of the glenoid labrum. J Shoulder Elbow Surg. 1996; 5:132–138. [PubMed: 8742877]
3. Chang EY, Fliszar E, Chung CB. Superior labrum anterior and posterior lesions and microinstability. Magn Reson Imaging Clin N Am. 2012; 20:277–294. x–xi. [PubMed: 22469404]
4. Cooper DE, Arnoczky SP, O'Brien SJ, et al. Anatomy, histology, and vascularity of the glenoid labrum. An anatomical study. J Bone Joint Surg Am. 1992; 74:46–52. [PubMed: 1734013]
5. Petersen W, Petersen F, Tillmann B. Structure and vascularization of the acetabular labrum with regard to the pathogenesis and healing of labral lesions. Arch Orthop Trauma Surg. 2003; 123:283–288. [PubMed: 12802599]
6. Chang EY, Du J, Chung CB. UTE imaging in the musculoskeletal system. J Magn Reson Imaging. 2015; 41:870–883. [PubMed: 25045018]
7. Groh MM, Herrera J. A comprehensive review of hip labral tears. Curr Rev Musculoskelet Med. 2009; 2:105–117. [PubMed: 19468871]
8. Connell DA, Potter HG, Wickiewicz TL, et al. Noncontrast magnetic resonance imaging of superior labral lesions. 102 cases confirmed at arthroscopic surgery. Am J Sports Med. 1999; 27:208–213. [PubMed: 10102103]
9. Connolly KP, Schwartzberg RS, Reuss B, et al. Sensitivity and specificity of noncontrast magnetic resonance imaging reports in the diagnosis of type-II superior labral anterior-posterior lesions in the community setting. J Bone Joint Surg Am. 2013; 95:308–313. [PubMed: 23426764]
10. Kim YJ, Choi JA, Oh JH, et al. Superior labral anteroposterior tears: accuracy and interobserver reliability of multidetector CT arthrography for diagnosis. Radiology. 2011; 260:207–215. [PubMed: 21518776]
11. Dinauer PA, Flemming DJ, Murphy KP, et al. Diagnosis of superior labral lesions: comparison of noncontrast MRI with indirect MR arthrography in unexercised shoulders. Skeletal Radiol. 2007; 36:195–202. [PubMed: 17139503]
12. Bencardino JT, Beltran J, Rosenberg ZS, et al. Superior labrum anterior-posterior lesions: diagnosis with MR arthrography of the shoulder. Radiology. 2000; 214:267–271. [PubMed: 10644135]
13. Williams A, Qian Y, Bear D, et al. Assessing degeneration of human articular cartilage with ultra-short echo time (UTE) T2* mapping. Osteoarthritis Cartilage. 2010; 18:539–546. [PubMed: 20170769]
14. Du J, Carl M, Diaz E, et al. Ultrashort TE T1rho (UTE T1rho) imaging of the Achilles tendon and meniscus. Magn Reson Med. 2010; 64:834–842. [PubMed: 20535810]

15. Biswas R, Bae W, Diaz E, et al. Ultrashort echo time (UTE) imaging with bi-component analysis: bound and free water evaluation of bovine cortical bone subject to sequential drying. Bone. 2012; 50:749–755. [PubMed: 22178540]
16. Bydder GM, Young IR. Clinical Use of the Partial Saturation and Saturation Recovery Sequences in Mr Imaging. Journal of Computer Assisted Tomography. 1985; 9:1020–1032. [PubMed: 4056131]
17. Du J, Carl M, Bydder M, et al. Qualitative and quantitative ultrashort echo time (UTE) imaging of cortical bone. J Magn Reson. 2010; 207:304–311. [PubMed: 20980179]
18. Yao L, Sinha S, Seeger LL. Mr Imaging of Joints - Analytic Optimization of Gre Techniques at 1.5-T. American Journal of Roentgenology. 1992; 158:339–345. [PubMed: 1370362]
19. Disler DG, Peters TL, Muscoreil SJ, et al. Fat-suppressed spoiled GRASS imaging of knee hyaline cartilage: technique optimization and comparison with conventional MR imaging. AJR Am J Roentgenol. 1994; 163:887–892. [PubMed: 8092029]
20. Wright P, Jellus V, McGonagle D, et al. Comparison of two ultrashort echo time sequences for the quantification of T1 within phantom and human Achilles tendon at 3 T. Magn Reson Med. 2012; 68:1279–1284. [PubMed: 22246857]
21. Dardzinski BJ, Mosher TJ, Li S, et al. Spatial variation of T2 in human articular cartilage. Radiology. 1997; 205:546–550. [PubMed: 9356643]
22. David-Vaudey E, Ghosh S, Ries M, et al. T2 relaxation time measurements in osteoarthritis. Magn Reson Imaging. 2004; 22:673–682. [PubMed: 15172061]
23. Buck FM, Bae WC, Diaz E, et al. Comparison of T1rho Measurements in Agarose Phantoms and Human Patellar Cartilage Using 2D Multislice Spiral and 3D Magnetization Prepared Partitioned k-Space Spoiled Gradient-Echo Snapshot Techniques at 3 T. American Journal of Roentgenology. 2011; 196:W174–W179. [PubMed: 21257859]
24. Li X, Han ET, Busse RF, et al. In vivo T(1rho) mapping in cartilage using 3D magnetization-prepared angle-modulated partitioned k-space spoiled gradient echo snapshots (3D MAPSS). Magn Reson Med. 2008; 59:298–307. [PubMed: 18228578]
25. Du J, Statum S, Znamirowski R, et al. Ultrashort TE T1rho magic angle imaging. Magn Reson Med. 2013; 69:682–687. [PubMed: 22539354]
26. Hargreaves BA, Gold GE, Beaulieu CF, et al. Comparison of new sequences for high-resolution cartilage imaging. Magn Reson Med. 2003; 49:700–709. [PubMed: 12652541]
27. Robson MD, Gatehouse PD, Bydder M, et al. Magnetic resonance: an introduction to ultrashort TE (UTE) imaging. J Comput Assist Tomogr. 2003; 27:825–846. [PubMed: 14600447]
28. Huber WP, Putz RV. Periarticular fiber system of the shoulder joint. Arthroscopy. 1997; 13:680–691. [PubMed: 9442320]
29. Jenkins JPR, Hickey DS, Zhu XP, et al. Mr Imaging of the Intervertebral-Disk - a Quantitative Study. British Journal of Radiology. 1985; 58:705–709. [PubMed: 3022862]
30. Andreisek G, White LM, Yang Y, et al. Delayed Gadolinium-enhanced MR Imaging of Articular Cartilage: Three-dimensional T1 Mapping with Variable Flip Angles and B-1 Correction. Radiology. 2009; 252:865–873. [PubMed: 19703855]
31. Duvvuri U, Reddy R, Patel SD, et al. T1rho-relaxation in articular cartilage: effects of enzymatic degradation. Magn Reson Med. 1997; 38:863–867. [PubMed: 9402184]
32. Rauscher I, Stahl R, Cheng J, et al. Meniscal measurements of T1rho and T2 at MR imaging in healthy subjects and patients with osteoarthritis. Radiology. 2008; 249:591–600. [PubMed: 18936315]
33. McNicol D, Roughley PJ. Extraction and characterization of proteoglycan from human meniscus. Biochem J. 1980; 185:705–713. [PubMed: 6892987]
34. Regatte RR, Akella SV, Lonner JH, et al. T1rho relaxation mapping in human osteoarthritis (OA) cartilage: comparison of T1rho with T2. J Magn Reson Imaging. 2006; 23:547–553. [PubMed: 16523468]
35. Fullerton GD, Cameron IL, Ord VA. Orientation of tendons in the magnetic field and its effect on T2 relaxation times. Radiology. 1985; 155:433–435. [PubMed: 3983395]

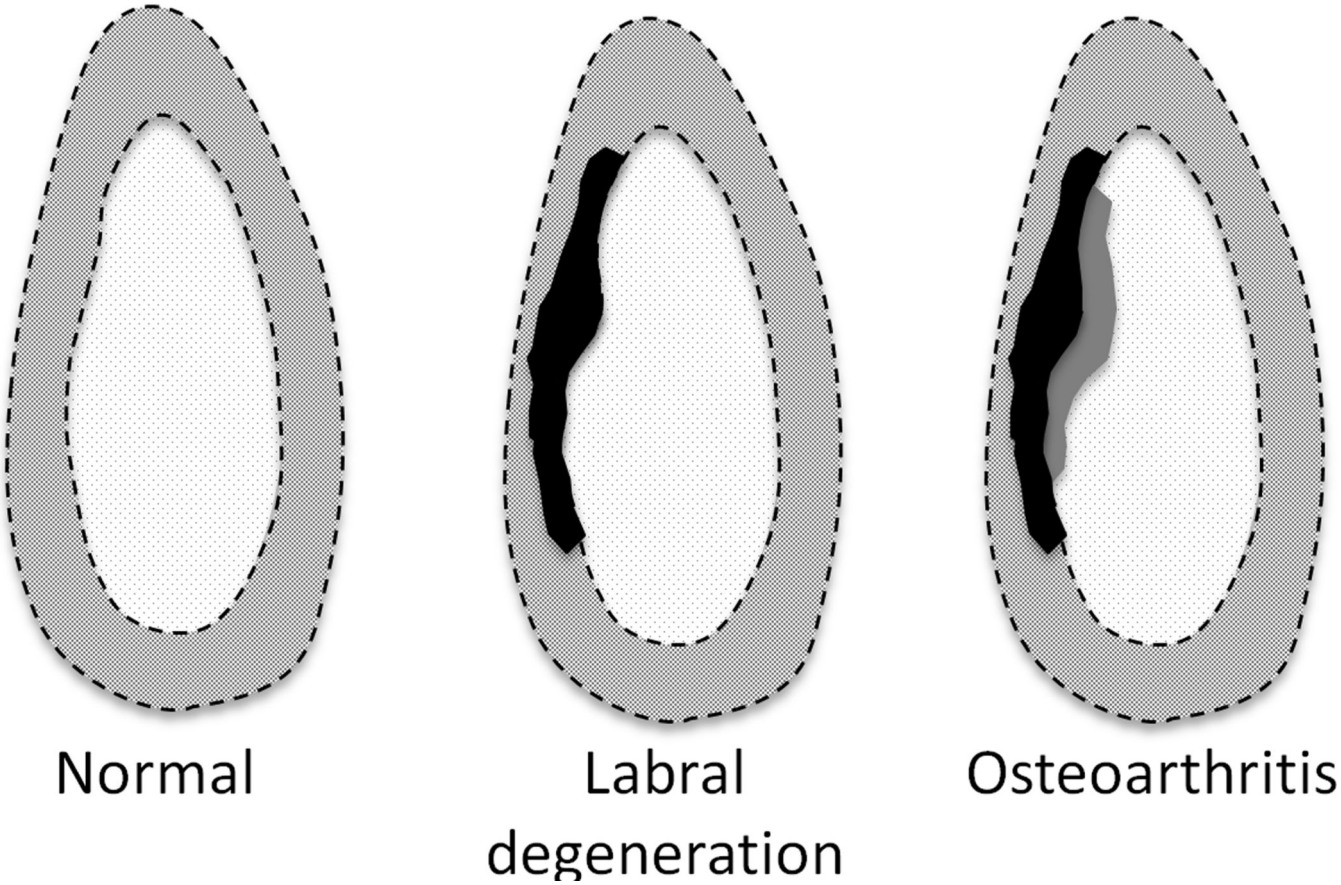

Figure 1.
Classification with gross inspection

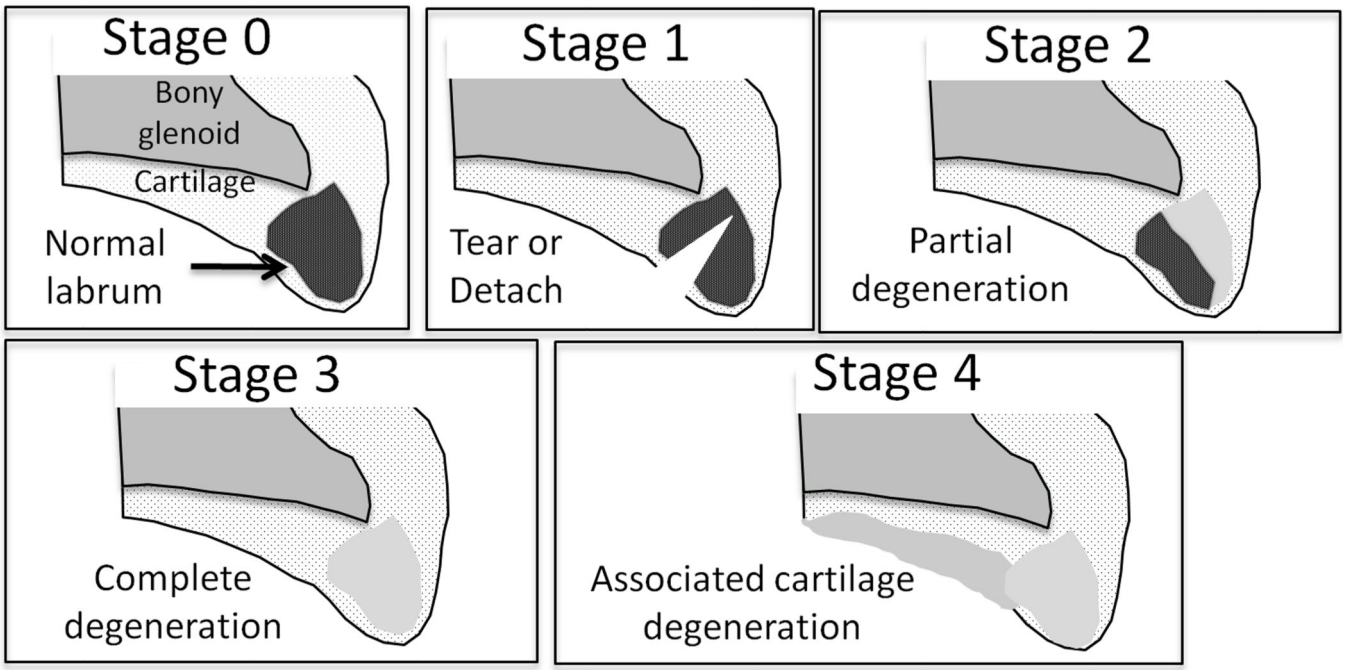

Figure 2.
Staging with MR images inspection

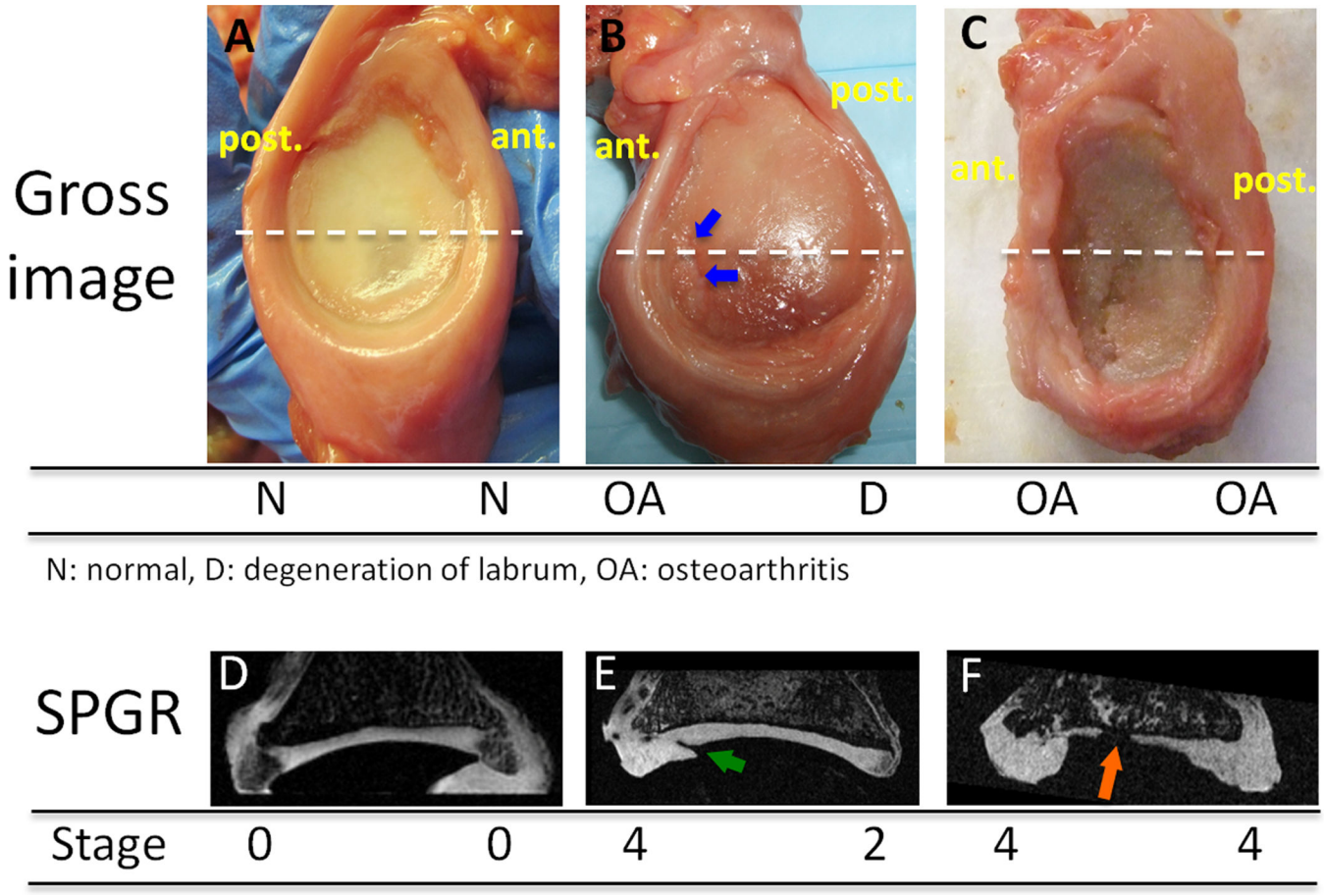

Figure 3.

A, B and C are photographs of three specimens demonstrating gross inspection findings (The dashed lines indicate the location of the axial SPGR MR images used for morphologic evaluation). (A): Both the labrum and articular cartilage are normal in this specimen obtained from a 41 year-old-female donor. (B): Anterior labrum thinned and reddish. The articular cartilage under the anterior part is degenerated (blue arrows). The posterior labrum appears degeneration. This specimen was obtained from a 94-year-old male donor. (C): Both the labrum and the glenoid cartilage is severely degenerated. This specimen was obtained from an 86-year-old female donor. D, E and F are axial fat saturated (FS) SPGR MR images of the glenoid labrum used for staging. (D): The labrum is triangular and hypointense. (E): The posterior labrum has both part of hyperintensity and part of hypointensity. It was classified as stage 2. The anterior labrum is diffusely hyperintense and is torn at the labral-cartilage junction (green arrow). It was classified as stage 4. (F): There is thickening, hyperintensity and loss of normal morphology at both anterior and posterior labrum. The glenoid cartilage appears irregular, thinned and has a central defect (orange arrow).

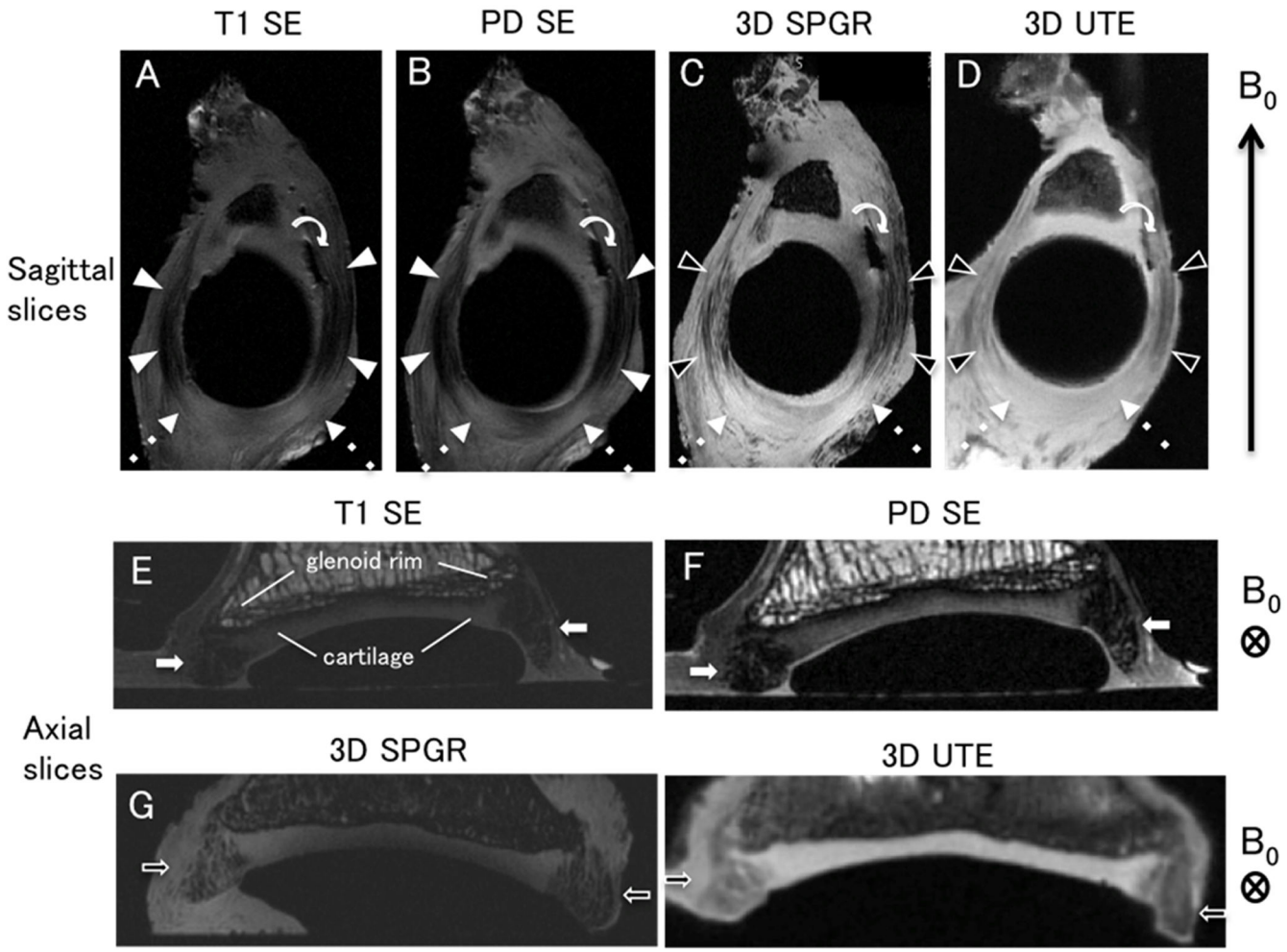

Figure 4.

Sagittal (upper row) and axial (middle and lower rows) high-resolution morphologic MR images of normal labral tissue. A well-defined defect probably ex-vivo is seen in the posterosuperior labrum (curved arrows). On T1 SE (A) and PD SE (B) sequences the anterior and posterior labrum appear hypointense (white arrowheads), while on 3D SPGR (C) and 3D UTE sequences (D), signal intensity of the labrum appears higher (open arrowheads). Focal areas of increased signal intensity (dashed arrows) secondary to magic angle effects are demonstrated. The signal intensity of the labrum is higher on 3D SPGR (G) and 3D UTE sequences (H) as compared with T1 (E) and PD sequences (F). Internal fiber structure of the labrum (white and open arrows) is better demonstrated on the 3D SGPR and 3D UTE sequences.

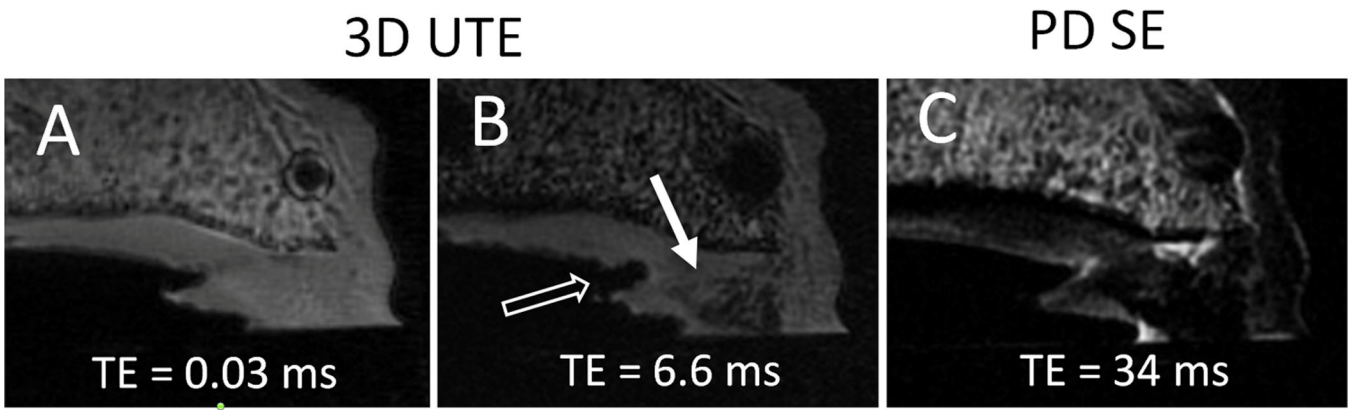

Figure 5.

3D UTE (TEs 0.03 and 6.6) and PD SE (TE 34 ms) demonstrate the internal fiber structure of an abnormal anterior labrum. The labrum is torn (open arrow) and there is a focal area of hyperintensity next to the tear (white arrow). The focal area of increased signal intensity (white arrow) is better demonstrated in the 3D UTE MR image with TE of 6.6 ms (B) where the contrast between the fibrocartilaginous matrix and the collagen fiber network of the labrum is greater. The fibrocartilaginous matrix appears hyperintense on the UTE MR images with shorter TEs and the focal area of altered signal intensity is masked (A).

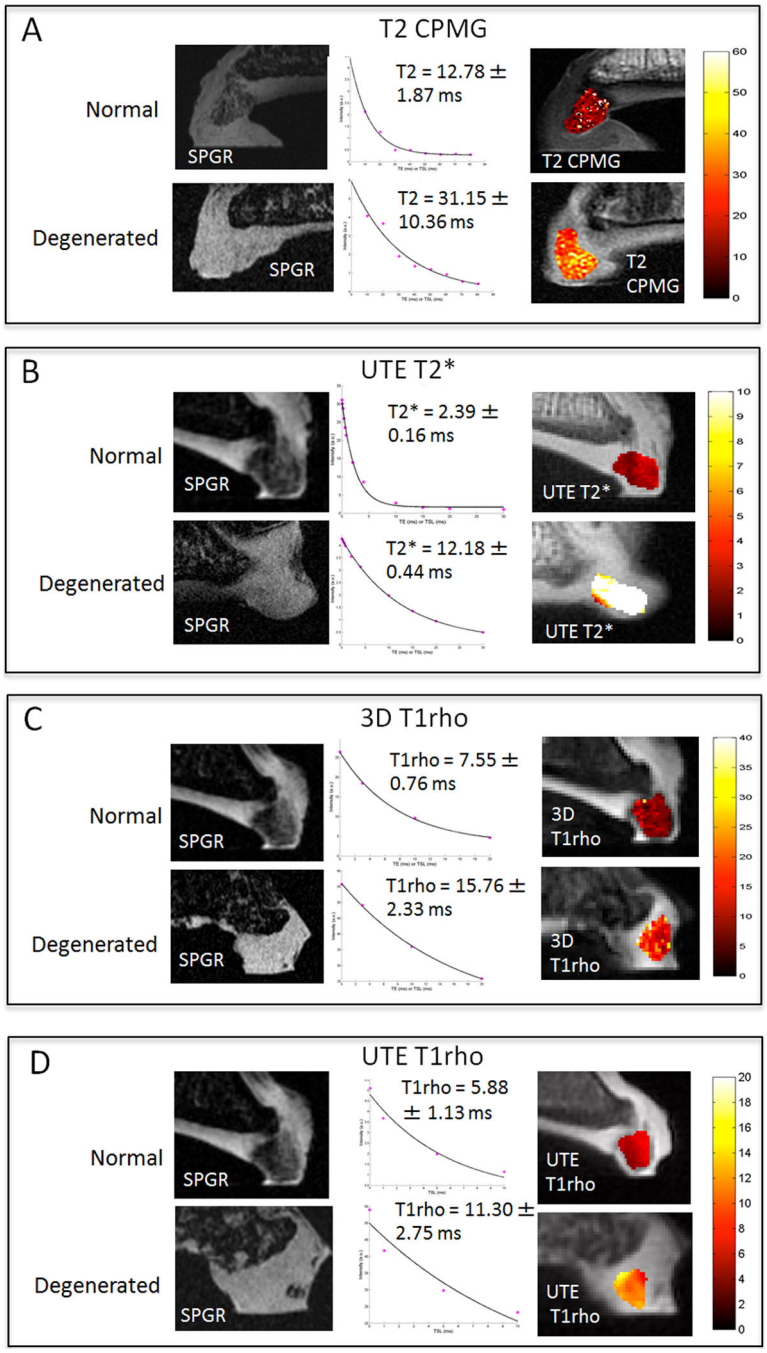

Figure 6.

High-resolution quantitative MR imaging of normal and degenerated labra. Axial SPGR MR images (left), mono-exponential fitting curves (center) and color maps (right) are shown. (A): Signal intensity and morphologic changes between a normal and a degenerated labrum are shown in this SPGR sequences. Increased signal intensity on T2 CPMG sequence is reflected in the mono-exponential fitting curves and the color mapping where the degenerated labrum has a higher mean T2 value. (B): Signal intensity differences between a normal and a degenerated labrum are also demonstrated on these SPGR sequences. Mono-

exponential fitting curves and color maps reflect the morphologic findings showing increased UTE T2* mean values as labrum degenerates. (C): The mean T1rho value on 3D T1rho sequence is also increased in the degenerated labrum. (D): The mean T1rho value on UTE T1rho sequence is also increased in the degenerated labrum.

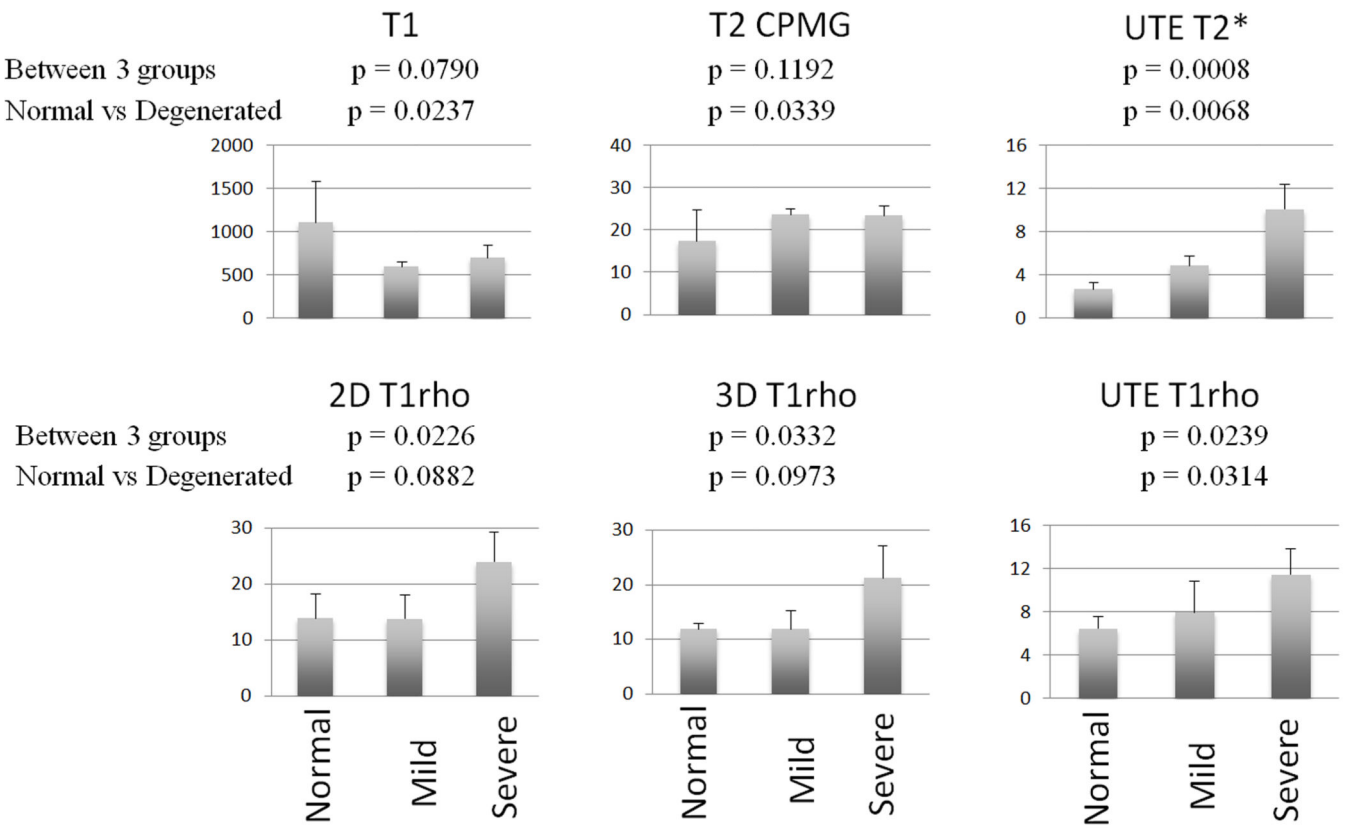

Figure 7.

The mean values from 3 groups (normal, mild degeneration and severe degeneration). Two kinds of p value are shown: the difference between 3 groups and normal vs degenerated (mild + severe) labra.

Table 1

Qualitative and Quantitative MRI Pulse Sequence Parameters

Sequence	TR	TE	NEX	Matrix	ST (mm)	Gap (mm)	Slices	FOV (cm)	FA	B/W
T1 SE	666.7	11	4	320 × 320	0.7	0	8	8 × 8	90	19.2
PD SE	2500	24	4	320 × 320	0.7	0	12	8 × 8	90	31.2
2D SPGR	200	4.1	6	384 × 384	0.9	0.5	8	8 × 8	44	31.2
3D SPGR	100	3.4	10	320 × 320	0.2	0	86	6 × 4	28	31.2
2D UTE	500	0.03, 8.8	2	512 × 511	1.7	0.7	3	8 × 8	40	41.7
3D UTE	250	0.03, 6.6	1	320 × 320	0.2	0	320	6 × 6	43	31.2
T1 TSR	TI: 26, 36, 66, 116, 216, 416, 816, 1216	0.01	2	192 × 191	3	0.6	1	6 × 6	40	31.3
T2 CPMG	2000	10.1, 20.2, 30.4, 40.4, 50.4, 60.5, 70.6, 80.7	1	320 × 256	3	0.6	1	6 × 6	90	41.7
UTE T2*	100	0.01, 0.1, 0.2, 0.4, 0.6, 0.8, 2, 4, 10, 15, 20, 30	2	256 × 255	3	0.6	1	6 × 6	28	31.3
2D-T1rho	1500	TSL: 0.02, 10,20,40	2	1024 × 85	3	0.6	1	6 × 6	90	125.0
3D-T1rho	8.7	TSL: 0.02,3,10,20	1	256 × 256	3	0	12	8 × 8	40	31.3
UTE-T1rho	400	TSL: 0.02, 1, 5, 10	2	192 × 191	3	0.6	1	6 × 6	40	31.2

ST: Slice thickness, FOV: Field of view, FA: Flip angle, B/W: Band width, SE: Spin echo, PD: proton density, SPGR: spoiled gradient echo, UTE: Ultra-short echo time, TI: time of inversion, TSL: time of spin locked pulse, TSR: total saturation recovery

Table 2

Gross and MRI Classification of Labra

Labrum No.	**1**		**2**		**3**		**4**		**5**		**6**	
ROI	**Ant.**	**Post.**	**Ant.**	**Post.**	**Ant.**	**Post.**	**Ant.**	**Post.**	**Ant.**	**Post.**	**Ant.**	**Post.**
Gross image stage	N	N	D	D	OA	D	OA	OA	D	N	OA	OA
MRI stage	0	0	3	2	4	2	4	4	3	0	4	4

ROI: Region of interests, Ant.: Anterior, Post. : Posterior
N: Normal, D: Degenerated, OA: Osteoarthritis